Published in final edited form as:
J Am Chem Soc. 2012 April 18; 134(15): 6878–6884. doi:10.1021/ja301812p.

Vibrational Analysis of Mononitrosyl Complexes in Hemerythrin and Flavodiiron Proteins: Relevance to Detoxifying NO Reductase

Takahiro Hayashi[†,||], **Jonathan D. Caranto**[‡], **Hirotoshi Matsumura**[†], **Donald M. Kurtz Jr.**[‡], and **Pierre Moënne-Loccoz**[†,*]

[†]Division of Environmental and Biomolecular Systems, Institute of Environmental Health, Oregon Health and Science University, 20,000 NW Walker Road, Beaverton, Oregon 97006-8921, USA

[‡]Department of Chemistry, University of Texas at San Antonio, San Antonio, Texas 78249, USA

Abstract

Flavodiiron proteins (FDPs) play important roles in the microbial nitrosative stress response in low-oxygen environments by reductively scavenging nitric oxide (NO). Recently, we showed that FMN-free diferrous FDP from *Thermotoga maritima* exposed to 1 equiv NO forms a stable diiron-mononitrosyl complex (deflavo-FDP(NO)) that can react further with NO to form N_2O [Hayashi, T.; Caranto, J. D.; Wampler, D. A.; Kurtz, D. M., Jr.; Moënne-Loccoz, P. *Biochemistry* **2010**, *49*, 7040–7049]. Here we report resonance Raman and low-temperature photolysis FTIR data that better define the structure of this diiron-mononitrosyl complex. We first validate this approach using the stable diiron-mononitrosyl complex of hemerythrin, Hr(NO), for which we observe a ν(NO) at 1658 cm^{-1}, the lowest ν(NO) ever reported for a nonheme $\{FeNO\}^7$ species. Both deflavo-FDP(NO) and the mononitrosyl adduct of the flavinated FPD (FDP(NO)) show ν(NO) at 1681 cm^{-1}, which is also unusually low. These results indicate that, in Hr(NO) and FDP(NO), the coordinated NO is exceptionally electron rich, more closely approaching the Fe(III)(NO^-) resonance structure. In the case of Hr(NO), this polarization may be promoted by steric enforcement of an unusually small FeNO angle, while in FDP(NO), the Fe(III)(NO^-) structure may be due to a semi-bridging electrostatic interaction with the second Fe(II) ion. In Hr(NO), accessibility and steric constraints prevent further reaction of the diiron-mononitrosyl complex with NO, whereas in FDP(NO) the increased nucleophilicity of the nitrosyl group may promote attack by a second NO to produce N_2O. This latter scenario is supported by theoretical modeling [Blomberg, L. M.; Blomberg, M. R.; Siegbahn, P. E. *J. Biol. Inorg. Chem.* **2007**, *12*, 79–89]. Published vibrational data on bioengineered models of denitrifying heme-nonheme NO reductases[Hayashi, T.; Miner, K. D.; Yeung, N.; Lin, Y.-W.; Lu, Y.; Moënne-Loccoz, P. *Biochemistry* **2011**, *50*, 5939–5947] support a similar mode of activation of a heme $\{FeNO\}^7$ species by the nearby nonheme Fe(II).

[*]Corresponding author: Pierre Moënne-Loccoz, Institute of Environmental Health, Oregon Health & Science University, 20,000 NW Walker Road, Beaverton, Oregon 97006. Tel: 503-748-1673; Fax: 503-748-1464. ploccoz@ebs.ogi.edu.
[||]Current address: Department of Synthetic Chemistry and Biological Chemistry, Graduate School of Engineering, Kyoto University, Katsura, Kyoto 615-8510, Japan.

Low-temperature RR spectra of 13C-labeled deoxy-Hr and its NO-adduct obtained with 647- and 458-nm excitations, low-temperature FTIR difference spectra of Hr(NO), ^{13}C-Hr(NO), deflavo-FDP(NO), FDP(NO), semi-reduced and fully reduced FDP. This material is available free of charge via Internet at http:/pubs.acs.org.

INTRODUCTION

Flavodiiron proteins (FDPs)[1] are widespread among microaerobic and anaerobic bacteria, archaea, and protozoan pathogens. Many FDPs provide protection against nitrosative stress by reductively scavenging NO to N_2O.1–8 This NO-reductase reaction occurs at a carboxylate-bridged nonheme diiron sites proximal to a flavin mononucleotide (FMN) cofactor located across the homodimer subunit interface (Figure 1). In a previous study, we demonstrated that the diferrous site of an FMN-free FDP from *Thermotoga maritima* (*Tm* deflavo-FDP) (Figure 1) is capable of a single turnover of 2 NO to N_2O in the presence of excess NO, albeit at a substoichiometric level since only ~0.7 equiv of N_2O formed per deflavo-FDP diiron site.9 In that same study, we further demonstrated that addition of one equiv NO per diferrous site results in essentially quantitative formation of a stable mononitrosyl adduct, which displays characteristic nitrosyl-to-iron LMCT absorptions at 420, 455, and 638 nm and a broad axial $g \sim 2$ EPR signal only observable below 30 K. This EPR spectrum is clearly distinct from the $g \sim 4$ resonances typically associated with nonheme $S = 3/2$ $\{FeNO\}^7$ species.[10] Instead, the $g \sim 2$ EPR signal is consistent with a ground-state $S = 1/2$ system arising from antiferromagnetic coupling of an $S = 3/2$ $\{FeNO\}^7$ with an $S = 2$ high-spin Fe(II).[9] This description is reminiscent of that reported for the mononitrosyl adduct of the diferrous (deoxy) form of the O_2-carrying nonheme diiron protein hemerythrin (Hr(NO)).[11,12] Relevant structural features of the Hr diiron site are included in Figure 1. Our results with *Tm* deflavo-FDP suggested a catalytic mechanism starting with the formation of the diiron-mononitrosyl adduct [Fe^{II}•$\{FeNO\}^7$], followed by the reaction of a second NO molecule to produce N_2O and a diferric site. In the flavinated enzyme (FDP), the differic site is then re-reduced by the proximal $FMNH_2$ cofactor (Scheme 1).

Here, we report that the diiron-mononitrosyl complex is also observed in the flavinated enzyme, FDP(NO), and we further characterize this [Fe^{II}•$\{FeNO\}^7$] cluster using FTIR spectroscopy. We also reexamine the vibrational spectra of Hr(NO), the only other known nonheme diiron-mononitrosyl complex. Previous resonance Raman (RR) studies of Hr(NO) identified the ν(FeNO) and δ(FeNO) modes from the $\{FeNO\}^7$ chromophore, but did not assign an N-O stretching vibration.[11,12] Our RR and FTIR experiments reveal that the [Fe^{II}•$\{FeNO\}^7$] complexes in Hr(NO) and in FDP(NO) exhibit exceptionally low ν(NO) frequencies compared to those of $\{FeNO\}^7$ species in other nonheme iron proteins and synthetic complexes.[9,13] Implications of these ν(NO) frequencies for the NO reduction mechanism of carboxylate-bridged diiron proteins are discussed.

EXPERIMENTAL PROCEDURES

Protein preparations

All protein concentrations are given in terms of nonheme diiron monomer. The expression and purification of recombinant *Phascolopsis gouldii* Hr was carried out as described previously.[14] ^{13}C-labeled Hr was expressed using the same procedure as that for unlabeled protein with minor modifications: a single colony of freshly transformed cells of the Hr overexpression strain[14] was cultured overnight in 50 mL of Luria-Bertani medium containing ampicillin. The cells were centrifuged at 4000 rpm for 10 min and resuspended

[1]Abbreviations: FDP, flavodiiron protein; deflavo-FDP, flavin-free FDP; FDP(NO), mononitrosyl adduct of diferrous FDP; deflavo-FDP$(NO)_2$, dinitrosyl adduct of flavin-free diferrous FDP; *Tm*, *Thermotoga maritima*; Hr, hemerythrin; deoxyHr, diferrous Hr; oxyHr, O_2 adduct of diferrous Hr; NROR, NADH:rubredoxin oxidoreductase; Rd, rubredoxin; MOPS, 3-(N-morpholino)propanesulfonic acid; diethylamine NONOate, diethylammonium (Z)-1-(N,N-diethylamino)diazen-1-ium-1,2-diolate; RR, resonance Raman; FTIR, Fourier transform infrared spectroscopy; EPR, electron paramagnetic resonance spectroscopy; R2, ribonucleotide reductase R2 protein; R2$(NO)_2$, dinitrosyl adduct of diferrous R2.

and cultured in 1.0 L of M9 medium containing ampicillin and 3 g of [$^{13}C_6$]-D-glucose (99%, Cambridge Isotope Laboratories, Inc. Andover MA) at 37 °C with shaking at 250 rpm. When the OD_{600} of the culture reached ~0.6, IPTG was added to a final concentration of 0.5 mM to induce overexpression of the Hr gene. The induced culture was incubated for another ~3.5 h at the same temperature and shaking speed, and the cells were subsequently harvested by centrifugation at 4000 rpm for 20 min. Cell lysis and protein purification were carried out as described previously. The expression and purification of recombinant *Tm* FDP, *Tm* rubredoxin (Rd), and *Tm* NADH:rubredoxin oxidoreductase (NROR) were performed as previously described.[15] *Tm* deflavo-FDP and the flavinated FDP were also prepared as described previously.[9]

Preparation of NO adducts

All manipulations were conducted in an anaerobic glovebox containing < 1 ppm of O_2 (Omnilab System, Vacuum Atmosphere Co.). Fully reduced (diferrous) deflavo-FDP and Hr were obtained either by titration to achieve a slight stoichiometric excess of sodium dithionite or by addition of excess dithionite followed by removal of the reducing agent with a desalting spin column (Zebra, Pierce). Complete reduction of FDP was achieved by overnight incubation of ~100 μM solutions in 50 mM MOPS pH 7.4, with 10 mM NADH, 4 μM Rd and 0.4 μM NROR; the excess NADH was removed after incubation using a desalting spin column inside the glove box. Stoichiometric addition of NO to fully reduced proteins was achieved by adding small aliquots of NO-saturated aqueous solutions prepared from NO gas previously treated with 1 M KOH solution to remove higher nitrogen oxide impurities. The concentration of NO in the stock solutions was determining by titration against deoxymyoglobin. Alternatively, diethylamine NONOate (Cayman Chemical, Ann Arbor, MI) was added to the reduced protein solutions. The concentration of the diethylamine NONOate stock solution was determined using an ε_{250} of 6500 $M^{-1}cm^{-1}$ in 0.01 M NaOH. Aliquot additions of diethylamine NONOate to a deoxymyoglobin control at pH~5 were used to further confirm the concentration of NO produced. In both cases, these additions were made just prior to transfer into EPR tubes, Raman capillaries or FTIR cells. Previously published UV-vis absorption spectra of Hr(NO)[11,12] and deflavo-FDP(NO)[9] were used to confirm the formation of the NO adducts.

Molecular spectroscopies

Electronic absorption spectra were obtained using a Cary 50 Varian spectrophotometer. Low temperature FTIR photolysis was performed as previously described with slight modifications.[9,16,17] Approximately 15 μL of ~1 mM protein solutions were deposited as a droplet on a CaF_2 window (International Crystal Labs, Garfield, NJ), and a second CaF_2 window was gently dropped on the sample to form an optical cell with a pathlength controlled by a 15-μm Teflon spacer (International Crystal Labs, Garfield, NJ). After confirming the presence of the NO adduct by UV-vis absorption spectroscopy, the FTIR cell was mounted to a sample rod which was then flash-frozen in liquid N_2, and inserted into the sample compartment of a closed-cycle cryogenic system (Omniplex, Advanced Research System).[9,16,17] This unit was placed inside the sample compartment of the FTIR and kept in the dark during the process of cooling to below 10 K. The temperature of the sample was monitored and controlled with a Cryo-Con 32 or a Lake Shore Model 331 unit. FTIR spectra were obtained on a Bruker Tensor 27 equipped with a liquid-N_2-cooled MCT detector. Sets of 1000-scan accumulations were acquired at 4-cm^{-1} resolution. Photolysis of nitrosyl complexes was performed by continuous illumination of the sample directly in the FTIR sample chamber using a 300-W arc lamp after filtering out heat and NIR emissions. The complete reversibility of all photolysis processes was confirmed by reproducing the same FTIR difference spectra after raising the sample temperature above 120 K, allowing rebinding of the photolyzed NO to the iron site.

Resonance Raman (RR) spectra were obtained on 1–2 mM protein solutions at either room temperature or 110 K using a custom McPherson 2061/207 spectrograph (set at 0.67 m with variable gratings) equipped with a liquid-N_2-cooled CCD detector (LN-1100PB, Princeton Instruments). The 458- and 647-nm excitations were derived from an Ar laser (Innova 90, Coherent) and a Kr laser (Innova 302, Coherent), respectively. Long-pass filters (RazorEdge, Semrock) were used to attenuate Rayleigh scattering. To assess the photosensitivity of the NO adduct, rapid acquisitions with a range of laser power and continuous sample translation or rotation were compared with longer data acquisitions on static samples. Frequencies were calibrated relative to indene and aspirin standards and are accurate to ±1 cm^{-1}. Polarization conditions were optimized using CCl_4 and indene. The integrity of the RR samples was confirmed by direct monitoring of their UV-vis absorption spectra in Raman capillaries before and after laser exposure.

Electron paramagnetic resonance (EPR) spectra were obtained with a Bruker E500 X-band EPR spectrometer equipped with a superX microwave bridge and a dual-mode cavity with a helium flow cryostat (ESR900, Oxford Instrument, Inc.). The experimental conditions, i.e., temperature, microwave power, and modulation amplitude, were varied to optimize the detection of all EPR-active species. Quantitation of the EPR signals was performed under non-saturating conditions by double integration and comparison with a series of Cu^{II}EDTA standards at varying concentrations. Photolysis of samples was achieved by direct illumination of samples in the EPR cavity using the same 300-W arc lamp used in the FTIR photolysis experiments. Typical protein concentrations for the EPR experiments were ~100 μM.

RESULTS

Characterization of Hr(NO)

Technological improvements in RR and FTIR spectroscopies prompted us to reexamine the Hr(NO) complex in search of the ν(NO) mode, which was not detected in the previous RR study.[12] Using a 647-nm laser excitation on Hr(NO) samples kept at cryogenic temperatures, we were able to reproduce the resonance-enhanced bands at 434 and 421 cm^{-1}, which in the previous study were assigned to ν(FeNO) and δ(FeNO) modes. Under these conditions, we also detect a band at 854 cm^{-1} that downshifts with ^{15}NO and $^{15}N^{18}O$ (Figure S1). We assign this latter band to a [ν(FeNO) + δ(FeNO)] combination mode by analogy with similar RR vibrations in other nonheme {FeNO}^{7} complexes.[9,13] Detection of the ν (NO) mode requires data collection on samples at room temperature or with blue rather than red laser excitations (Figure S2). The room temperature RR spectra of Hr(NO) obtained with a 458-nm excitation exhibit a band at 1671 cm^{-1} that downshifts to 1647 and 1587 cm^{-1} with ^{15}NO and $^{15}N^{18}O$, respectively (Figure 2). While the −24 cm^{-1} shift observed with ^{15}NO is smaller than the −30 cm^{-1} shift predicted for an isolated NO oscillator, the −84 cm^{-1} shift observed with $^{15}N^{18}O$ is larger than the −75 cm^{-1} shift predicted by Hooke's law. These discrepancies between observed and calculated shifts, and in particular, a greater than expected isotope shift, are suggestive of Fermi coupling of the ν(NO) mode with another vibration(s). Accordingly, in the RR difference spectra obtained by subtracting the spectrum of deoxy-Hr from that of Hr(NO), the ν(NO) band is accompanied by a nearby signal at ~1606 cm^{-1} (Figure 2). Based on FTIR data described below, this mode is assigned to a carboxylate ν_{as}(COO) mode. In agreement with this assignment, the Fermi coupling observed in the RR spectra of Hr(NO) is canceled by full ^{13}C-labeling of Hr (^{13}C-Hr) since the $\nu_{as}(^{13}COO)$ downshifts away from the ν(NO) mode. Specifically, the RR spectrum of ^{13}C-Hr(NO) shows an ν(NO) at 1671 cm^{-1} that downshifts to 1642 cm^{-1} with ^{15}NO, as expected for an isolated NO diatomic oscillator (Figure 2). Low-temperature RR spectra of Hr(NO) show that the ν(NO) mode is significantly affected by temperature as it downshifts

to 1661 cm^{-1} at 110 K; in contrast, the ν(FeNO) and δ(FeNO) frequencies show only modest upshifts at cryogenic temperatures (Figure S2).

As reported previously, Hr(NO) exhibits an axial $S = 1/2$ EPR signal with $g_{//}$ and $g_{\perp}$ near 2.78 and 1.80, respectively, arising from antiferromagnetic coupling between the $S = 3/2$ $\{FeNO\}^7$ and the $S = 2$ high-spin Fe(II).[11,12] Illumination of Hr(NO) at 4.2 K results in a loss of ~50 % of this EPR signal and in the appearance of a new resonance at $g = 1.96$ characteristic of free NO (Figure 3). These light-induced EPR changes are indicative of efficient photolysis of NO at cryogenic temperatures and are readily reverted by raising the sample temperature above 120 K to allow rebinding of NO at the diiron site.

Monitoring this photolysis process by FTIR spectroscopy using 'dark' minus 'illuminated' difference spectra reveals prominent positive bands at 1661, 1608, and 1398 cm^{-1} and smaller perturbations across the spectral range (Figure 4). The double difference FTIR spectrum, computed from the light-induced difference spectra of Hr(NO) and Hr(^{15}NO), isolates isotope-sensitive modes and cancels out many light-induced differential signals (Figure 4). The remaining signals are: i) the positive band at 1661 cm^{-1} that downshifts to 1637 cm^{-1} with ^{15}NO, assigned to the ν(NO) of the $\{FeNO\}^7$ complex, ii) a weak negative band at 1872 cm^{-1} that downshifts to 1839 cm^{-1}, assigned to the ν(NO) of the photolyzed NO docked within the protein matrix, and iii) the 1608 cm^{-1} positive band that downshifts 4 cm^{-1} to 1604 cm^{-1}, assigned to a carboxylate ν_{as}(COO). These assignments are also supported by FTIR spectra of Hr(15N18O) (Figure S3) and by experiments using uniformly ^{13}C-labeled Hr (^{13}C-Hr). Specifically, the differential signals at 1608 and 1398 cm^{-1} in Hr(NO) downshift to 1570 and 1367 cm^{-1} in ^{13}C-Hr(NO) as expected for ν_{as}(COO) and ν_s(COO), respectively, of a carboxylate group(s) (Figure 4). As the ^{13}C-labelling downshifts the ν_{as}(COO), it uncouples this mode from the ν (NO) of the $\{FeNO\}^7$ species which is now observed at 1658 cm^{-1} and exhibits a −28 cm^{-1} shift with ^{15}NO in agreement with the calculated shift for an isolated diatomic oscillator. These FTIR results nicely support those from the RR spectra reported above. The frequency gap between ν_{as}(COO) and ν_s(COO), denoted as $\Delta_{as\text{-}s}$, is > 200 cm^{-1} (Table 1). This $\Delta_{as\text{-}s}$ value is consistent with μ-1,3 bridging carboxylates,[18,19] which, based on the crystal structures of deoxy-Hr and its O_2 adduct (Figure 1),[20] is the expected coordination geometry for the only two carboxylate ligands in Hr(NO). Although the previous RR investigation reported that the ν(FeNO) and δ(FeNO) were sensitive to H_2O/D_2O exchange, we were not able to reproduce these observations in our RR spectra. Similarly, the FTIR spectra of Hr(NO) do not report any effect of H/D exchange on the ν(NO) mode (Figure S3).

Characterization of FDP(NO)

Addition of 1 equiv NO per diiron site to diferrous FDP or deflavo-FDP results in the formation of $S = 1/2$ [Fe^{II}•$\{FeNO\}^7$] complexes with axial $g \sim 2$ EPR signals (Figure 5). Double integration of these EPR signals against Cu^{II}EDTA standards indicates that they represent 0.8 spin per diiron site. While the EPR spectrum of FDP(NO) presents a well-resolved low-field resonance $g_{//}$ at 2.38 and a $g_{\perp}$ at ~1.9, the spectrum of deflavo-FDP(NO) appears broader with a $g_{//}$ at 2.30 and $g_{\perp}$ near 2.0. After illumination at low-temperature, the EPR spectrum of FDP(NO) shows a large drop in the intensity of the low-field resonance at $g = 2.38$; some unassigned signal appears to remain after illumination and new sharp EPR features appear, but these additional signals integrate to less than 10 % of diiron sites (Figure 5). Although illumination of deflavo-FDP(NO) also results in the loss of the $g_{//}$ and $g_{\perp}$ resonances, the EPR spectrum obtained after illumination displays more prominent features than in FDP(NO), and with the insight of the FTIR-photolysis data, these EPR data may reflect a greater heterogeneity in deflavo-FDP(NO).

As reported previously,[9] the RR spectrum of deflavo-FDP(NO) obtained with 458-nm excitation reveals a ν(FeNO) at 451 cm^{-1}, but detecting the ν(NO) mode was precluded by the higher background signal observed in the high-frequency region.

The low-temperature 'dark' minus 'illuminated' FTIR difference spectrum of deflavo-FDP(NO) shows a positive band at 1681 cm^{-1} that downshifts to 1652 cm^{-1} with ^{15}NO (Figure 6). Relatively intense differential signals centered at 1586 and 1421 cm^{-1} are good candidates for the ν_{as}(COO) and ν_{s}(COO) of a bridging carboxylate group,18,19,21 that is perturbed upon NO photolysis. As described for Hr(NO), the $\Delta_{as\text{-}s}$ value of 165 cm^{-1} suggests that these modes reflect perturbations of a bridging bidentate rather than terminal carboxylate ligand(s).[22] In deflavo-FDP($^{15}N^{18}O$), the ν(NO) splits into two bands of equal intensity at 1574 and 1624 cm^{-1}. The former frequency is below and the latter above the predicted 1605-cm^{-1} value for a ν ($^{15}N^{18}O$) diatomic oscillator, suggesting Fermi coupling of this mode, presumably with an ν_{as}(COO) as in the vibrational spectra of Hr(NO). Negative ν(NO) bands from the photolyzed NO are very weak, but nevertheless, clearly identified, including in double difference FTIR spectra that combine photolysis and NO-isotopic sensitivity (Figure S4).

The light-induced FTIR difference spectra of FDP(NO) (Figure 6) are very similar to those of deflavo-FDP(NO), with positive and negative bands at 1681 and 1869 cm^{-1}, respectively, and at 1652 and 1837 cm^{-1} in FDP(^{15}NO). As with deflavo-FDP($^{15}N^{18}O$), FDP($^{15}N^{18}O$) exhibits a split ν($^{15}N^{18}O$) at 1575/1624 cm^{-1} compared to its predicted value of 1605 cm^{-1} from Hooke's law. The differential signals assigned to ν_{as}(COO) and ν_{s}(COO) in the spectra of deflavo-FDP(NO), i.e., 1586 and 1421 cm^{-1}, respectively, are conserved in the spectra of FDP(NO). A shoulder at 1556 cm^{-1}, which is not observed in the spectra of deflavo-FDP(NO) or in control experiments with semi- or fully-reduced FDP (Figure S5), does not shift with NO isotope labeling and is tentatively assigned to a perturbation of the FMN cofactor. As with Hr(NO), the ν(NO)s of deflavo- and FDP(NO) are not affected by H/D exchange (Figure 6), indicating that the bound NO group is not involved in hydrogen bond interactions.

DISCUSSION

A striking observation from our results is that the [Fe^{II}•{FeNO}^{7}] complexes of both Hr(NO) and FDP(NO) show ν(NO)s that are significantly lower than those of all previously reported nonheme {FeNO}^{7} species (Table 1 and Figure 7). These low ν(NO)s suggest an unusually high π^* electron density at the nitrosyl group. The factors influencing the electronic distribution within nonheme $S = 3/2$ {FeNO}^{7} species between the limiting Fe(I)(NO^+) and Fe(III)(NO^-) formulations have been the subject of numerous studies.[23] Positively charged environments near the NO group, strong electron-donating ligands to the iron, and bent Fe-N-O unit can favor the Fe(III)(NO^-) resonance structure. The only reasonably close structurally characterized mimic of the diiron-dinitrosyl coordination spheres in deflavo-FDP$(NO)_2$ is $Fe_2(NO)_2$(Et-HPTB)$(O_2CPh)(BF_4)_2$, where two equivalent $S = 3/2$ {FeNO}^{7} centers are in distorted octahedral coordination geometries with three N ligands and two O ligands from bridging μ-alkoxo and μ-carboxylate ligands. The crystalline complex has FeNO angles of 167 ± 1°, and a single ν(NO) band at 1785 cm^{-1}.[24] Both the FeNO angle and NO stretching frequency are at the higher end of the range observed for $S = 3/2$ {FeNO}^{7} units. In contrast, the 6-coordinate $S = 3/2$ {FeNO}^{7} unit in Fe($S^{Me2}N_4$(tren))(NO)(OTf) exhibits an FeNO angle of 152° and a ν(NO) at 1685 cm^{-1}.[25] This 100-cm^{-1} decrease in ν(NO) is believed to reflect the strong electron-donating character of the thiolate ligand which shifts electron density from the Fe-NO bond to the π^* N-O orbital. Similar notions of competition between π donating ligands were put forth by Johnson and coworkers[26] to explain the apparent weakening of the *trans* Fe-S(Cys) bond in

the NO adduct of superoxide reductase (SOR) compared to the oxidized (ferric) enzyme. Crystal structures of SOR suggest that the thiolate S atom acts as a hydrogen bond acceptor, further weakening its electron-donation to the iron and allowing for strong electron-donation from the NO group in SOR(NO), as suggested by the high ν(NO) at 1721 cm^{-1}.[27] Lehnert and coworkers observed a correlation between ν(FeNO) and ν(NO) in nonheme $\{FeNO\}^7$ complexes with pyridyl, amine, and carboxylate ligands.[28] Their DFT calculations indicate that electron donation from anionic ligands inhibits NO $\pi^* \rightarrow$ Fe d_{xz} and d_{yz} donation, thereby weakening both Fe-N and N-O bonds and lowering their corresponding stretching frequencies.

We, therefore, consider the possibility that the low ν(NO)s in Hr(NO) and FDP(NO) reflect an unusually strong competition for ligand-to-metal π-electron donation by the protein ligands. Based on crystal structures and the magnetic coupling of their iron centers,[9,12,20] the coordination spheres of the$\{FeNO\}^7$ centers in Hr(NO) and FDP(NO) are expected to include two histidines, two carboxylate groups and a bridging solvent molecule, with the only apparent difference being a bridging versus terminal carboxylate ligand (Scheme 2). However, equivalent coordination spheres are also expected for the two $\{FeNO\}^7$ units in deflavo-FDP$(NO)_2$ but they do not show unusually low ν(NO) (Table 1). The relatively carboxylate-rich diiron site expected in the dinitrosyl adduct of the R2 protein from *Escherichia coli* ribonucleotide reductase (R2$(NO)_2$) also give rise to a "mid-range" ν(NO) at 1742 cm^{-1}.[13] The asymmetry of the diiron-mononitrosyl complexes in FDP(NO) and Hr(NO) relative to the diiron-dinitrosyl complexes in deflavo-FDP$(NO)_2$, R2$(NO)_2$ and $Fe_2(NO)_2$(Et-HPTB)$(O_2CPh)(BF_4)_2$ could conceivably allow electron donation from the Fe(II) center to the $\{FeNO\}^7$ center. However, Mössbauer spectra of Hr(NO) show a clearly resolved ferrous signal with no evidence for unusual electron donation from the Fe(II) to the $\{FeNO\}^7$ center.[12,29]

An alternative rationale may be that unusually small FeNO angles are stabilized in Hr(NO) and FDP(NO) because of steric constraints and semi-bridging electrostatic interactions between the $\{FeNO\}^7$ and Fe(II) centers (Scheme 2), thereby favoring the Fe(III)(NO^-) resonance structure and low ν(NO)s. In Hr(NO), NO is expected to bind to the same coordination site as does O_2 in oxyHr (Figure 1), and with six ligands to the Fe(II), five of which from the protein, a semi-bridging NO coordination is not likely, but a small FeNO angle could be enforced by the sterically confined pocket surrounding the O_2 coordination site.[14,20] Further bending of the FeNO unit upon thermal contraction of Hr(NO) may explain the 10-cm^{-1} downshift of the ν(NO) mode at cryogenic temperatures. Hydrogen bonding between the bridging solvent and coordinated NO could assist in stabilizing a small FeNO angle in Hr(NO) as occurs for coordinated O_2 in oxyHr. However, we could not detect a D_2O-isotope effect in the vibrational spectra of Hr(NO).

In contrast to Hr, crystal structures of several FDPs[6,7] indicate a more expansive binding pocket near the diiron site, making steric restrictions on the FeNO angle less likely. The crystal structures also suggest that the Fe(II) center in FDP(NO) would retain an open coordination site and may permit a semi-bridging interaction of NO within the $[Fe^{II}\bullet\{FeNO\}^7]$ unit. This type of interaction is, in fact, supported by DFT calculations.[30] The resulting electrostatic stabilization of electron density on the NO group of the $\{FeNO\}^7$ unit could account for the low ν(NO). This polarization towards the Fe(III)(NO^-) resonance structure would also increase the nucleophilicity of the coordinated NO, thereby promoting its reactivity towards a second NO to form a hyponitrite intermediate (Scheme 1), as suggested by the aforementioned DFT calculations. In the case of Hr(NO), the steric restrictions enforcing the low FeNO angle would also inhibit interaction with a second NO. The extent to which the mononitrosyl-to-hyponitrite mechanism shown in Scheme 1 competes with binding of a second NO to the unoccupied Fe(II) in FDP(NO) to form a

$[\{FeNO\}^7]_2$ unit analogous to that in our previously characterized deflavo-FDP$(NO)_2$ is still unclear.[9] Interestingly, we also observed unusually low ν(NO)s in engineered myoglobins when the heme $\{FeNO\}^7$ species is within a few angstroms from a distal nonheme iron(II) or Zn(II).[31] Asymmetric $[Fe^{II}•Fe^{III}(NO^-)]$ complexes may, thus, be common intermediates in the NO reductase activity of detoxifying, nonheme diiron, and denitrifying, heme-nonheme diiron enzymes.

Supplementary Material

Refer to Web version on PubMed Central for supplementary material.

Acknowledgments

This article is dedicated to the memory of Thomas and Joann Loehr. This work was supported by the National Institute of Health (GM074785 to P.M.-L., GM040388 to D.M.K., and MBRS/RISE GM060655 to J.D.C.) and a Vertex Pharmaceutical Scholarship for T.H. We thank Dr. Michiko Nakano for help with the expression and purification of ^{13}C-Hr.

References

1. Gardner AM, Helmick RA, Gardner PR. J Biol Chem. 2002; 277:8172. [PubMed: 11751865]
2. Gomes CM, Giuffre A, Forte E, Vicente JB, Saraiva LM, Brunori M, Teixeira M. J Biol Chem. 2002; 277:25273. [PubMed: 12101220]
3. Silaghi-Dumitrescu R, Coulter ED, Das A, Ljungdahl LG, Jameson GN, Huynh BH, Kurtz DM Jr. Biochemistry. 2003; 42:2806. [PubMed: 12627946]
4. Saraiva LM, Vicente JB, Teixeira M. Adv Microb Physiol. 2004; 49:77. [PubMed: 15518829]
5. Silaghi-Dumitrescu R, Kurtz DM Jr, Ljungdahl LG, Lanzilotta WN. Biochemistry. 2005; 44:6492. [PubMed: 15850383]
6. Kurtz DMJ. Dalton trans. 2007:4115.
7. Di Matteo A, Scandurra FM, Testa F, Forte E, Sarti P, Brunori M, Giuffre A. J Biol Chem. 2008; 283:4061. [PubMed: 18077462]
8. Le Fourn C, Brasseur G, Brochier-Armanet C, Pieulle L, Brioukhanov A, Ollivier B, Dolla A. Environ Microbiol. 2011
9. Hayashi T, Caranto JD, Wampler DA, Kurtz DM, Moënne-Loccoz P. Biochemistry. 2010; 49:7040. [PubMed: 20669924]
10. Brown CA, Pavlosky MA, Westre TE, Zhang Y, Hedman B, Hodgson KO, Solomon EI. J Am Chem Soc. 1995; 117:715.
11. Nocek JM, Kurtz DM Jr, Sage JT, Debrunner PG, Maroney MJ, Que L Jr. J Am Chem Soc. 1985; 107:3382.
12. Nocek JM, Kurtz DM Jr, Sage JT, Xia YM, Debrunner PG, Shiemke AK, Sanders-Loehr J, Loehr TM. Biochemistry. 1988; 27:1014. [PubMed: 3365363]
13. Lu S, Libby E, Saleh L, Xing G, Bollinger JM Jr, Moënne-Loccoz P. J Biol Inorg Chem. 2004; 9:818. [PubMed: 15311337]
14. Farmer CS, Kurtz DM Jr, Phillips RS, Ai J, Sanders-Loehr J. J Biol Chem. 2000; 275:17043. [PubMed: 10748012]
15. Hillmann F, Riebe O, Fischer RJ, Mot A, Caranto JD, Kurtz DM Jr, Bahl H. FEBS Lett. 2009; 583:241. [PubMed: 19084524]
16. Hayashi T, Lin IJ, Chen Y, Fee JA, Moënne-Loccoz P. J Am Chem Soc. 2007; 129:14952. [PubMed: 17997553]
17. Hayashi T, Lin MT, Ganesan K, Chen Y, Fee JA, Gennis RB, Moënne-Loccoz P. Biochemistry. 2009; 48:883. [PubMed: 19187032]
18. Costas M, Cady CW, Kryatov SV, Ray M, Ryan MJ, Rybak-Akimova EV, Que L Jr. Inorg Chem. 2003; 42:7519. [PubMed: 14606847]

19. Do LH, Hayashi T, Moënne-Loccoz P, Lippard SJ. J Am Chem Soc. 2010; 132:1273. [PubMed: 20055391]
20. Stenkamp RE. Chem Rev. 1994; 94:715.
21. Duprat AF, Traylor TG, Wu GZ, Coletta M, Sharma VS, Walda KN, Magde D. Biochemistry. 1995; 34:2634. [PubMed: 7873545]
22. Nara M, Tanokura M. Biochem Biophys Res Comm. 2008; 369:225. [PubMed: 18182161]
23. Sun N, Liu LV, Dey A, Villar-Acevedo G, Kovacs JA, Darensbourg MY, Hodgson KO, Hedman B, Solomon EI. Inorg Chem. 2010; 50:427.
24. Feig AL, Bautista MT, Lippard SJ. Inorg Chem. 1996; 35:6892. [PubMed: 11666858]
25. Villar-Acevedo G, Nam E, Fitch S, Benedict J, Freudenthal J, Kaminsky W, Kovacs JA. J Am Chem Soc. 2011; 133:1419. [PubMed: 21207999]
26. Clay MD, Cosper CA, Jenney FE Jr, Adams MW, Johnson MK. Proc Natl Acad Sci USA. 2003; 100:3796. [PubMed: 12655067]
27. Yeh AP, Hu Y, Jenney FE Jr, Adams MW, Rees DC. Biochemistry. 2000; 39:2499. [PubMed: 10704199]
28. Berto TC, Hoffman MB, Murata Y, Landenberger KB, Alp EE, Zhao J, Lehnert N. J Am Chem Soc. 2011
29. Rodriguez JH, Xia YM, Debrunner PG. J Am Chem Soc. 1999; 121:7846.
30. Blomberg LM, Blomberg MR, Siegbahn PE. J Biol Inorg Chem. 2007; 12:79. [PubMed: 16957917]
31. Hayashi T, Miner KD, Yeung N, Lin YW, Lu Y, Moënne-Loccoz P. Biochemistry. 2011; 50:5939. [PubMed: 21634416]
32. Frazao C, Silva G, Gomes CM, Matias P, Coelho R, Sieker L, Macedo S, Liu MY, Oliveira S, Teixeira M, Xavier AV, Rodrigues-Pousada C, Carrondo MA, Le Gall J. Nat Struct Biol. 2000; 7:1041. [PubMed: 11062560]

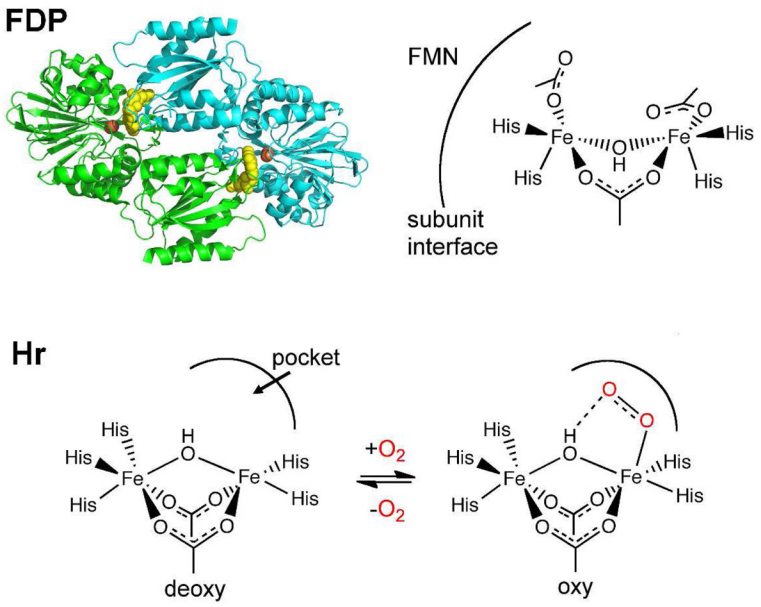

Figure 1.

Backbone structure of *Tm* deflavo-FDP homodimer (green and blue ribbons, PDB entry 1VME). The iron atoms are depicted as orange spheres. Because a crystal structure of flavinated *Tm* FDP is not available, the FMN cofactor (yellow spheres) is from a backbone superposition of *desulfovibrio gigas* FDP (PDB entry 1E5D).[32] Drawing generated in PyMOL (Delano Scientific, Inc.). Also shown as schematic structures of the consensus diiron site in FDPs (top right) and the diiron sites of deoxy and oxyHr (bottom schemes).

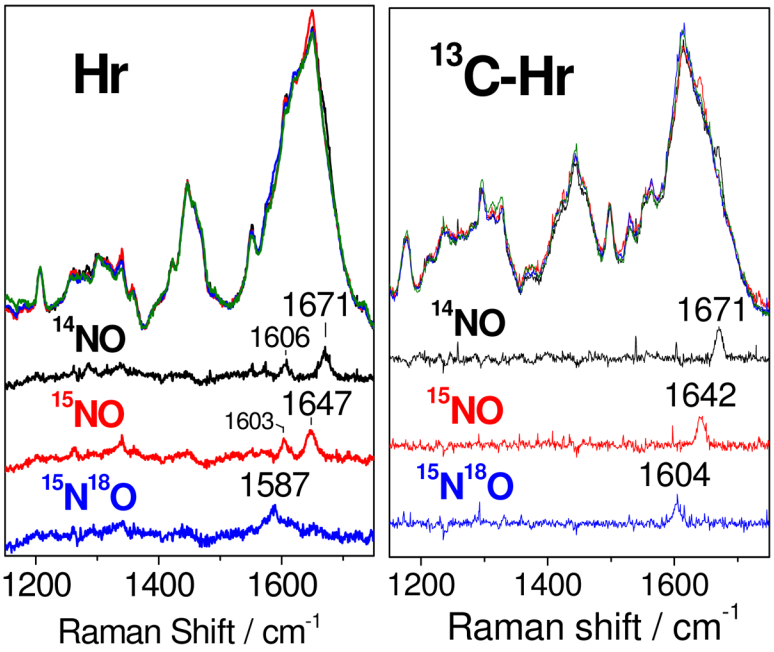

Figure 2.

Room-temperature RR spectra of natural abundance and ^{13}C-labeled deoxy-Hr (green) and their NO adducts prepared with ^{14}NO (black), ^{15}NO (red), and ^{15}N^{18}O (blue) are superimposed above the corresponding NO adducts minus deoxy-Hr difference spectra. These spectra were obtained with a 458-nm laser excitation.

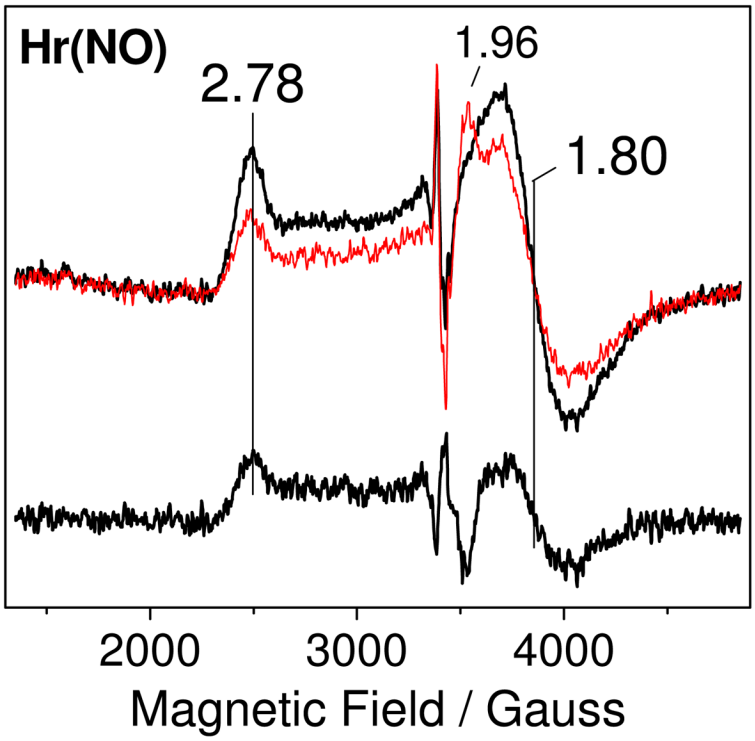

Figure 3.
EPR spectra of Hr(NO) before (black) and after (red) illumination, and dark minus illuminated difference spectra (bottom trace), obtained at 4.2 K. Conditions: protein concentration, 60 μM in 50 mM HEPES and 150 mM Na_2SO_4 (pH7.5); microwave frequency, 9.67 GHz; microwave power, 40 μW; modulation amplitude, 10 G.

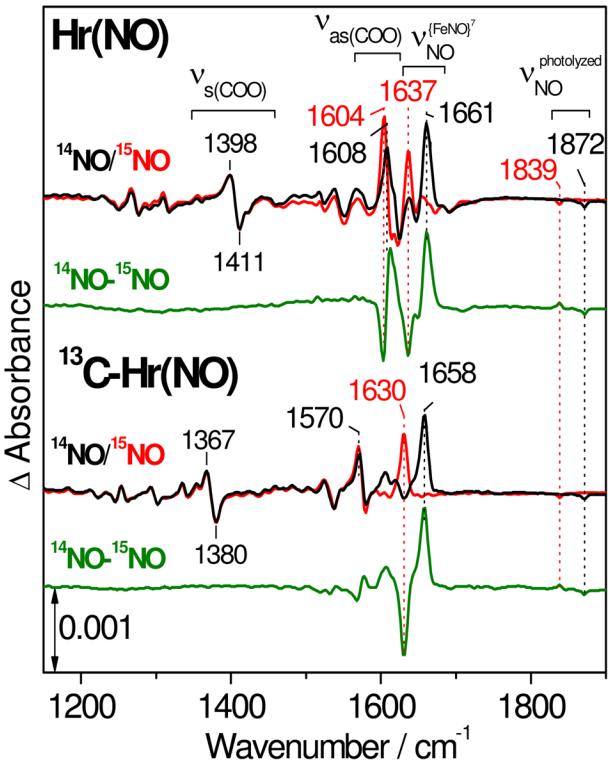

Figure 4.

FTIR dark minus illuminated difference spectra of Hr(NO) (top) and ^{13}C-Hr(NO) (bottom) with ^{14}NO (black) and ^{15}NO (red) at 20 K. Also shown are ^{14}NO minus ^{15}NO double-difference spectra (green).

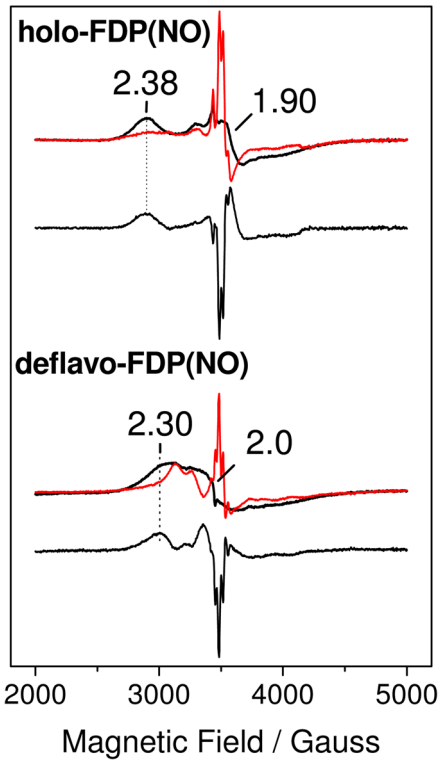

Figure 5.
EPR spectra of FDP(NO) (top) and deflavo-FDP(NO) (bottom) before (black) and after (red) illumination at 4.2 K. Also shown below each pair are the resulting dark minus illuminated difference spectra. Conditions: protein concentration, 100 μM in 50 mM MOPS (pH7.4); microwave frequency, 9.67 GHz; microwave power, 2 mW; modulation amplitude of 10 G.

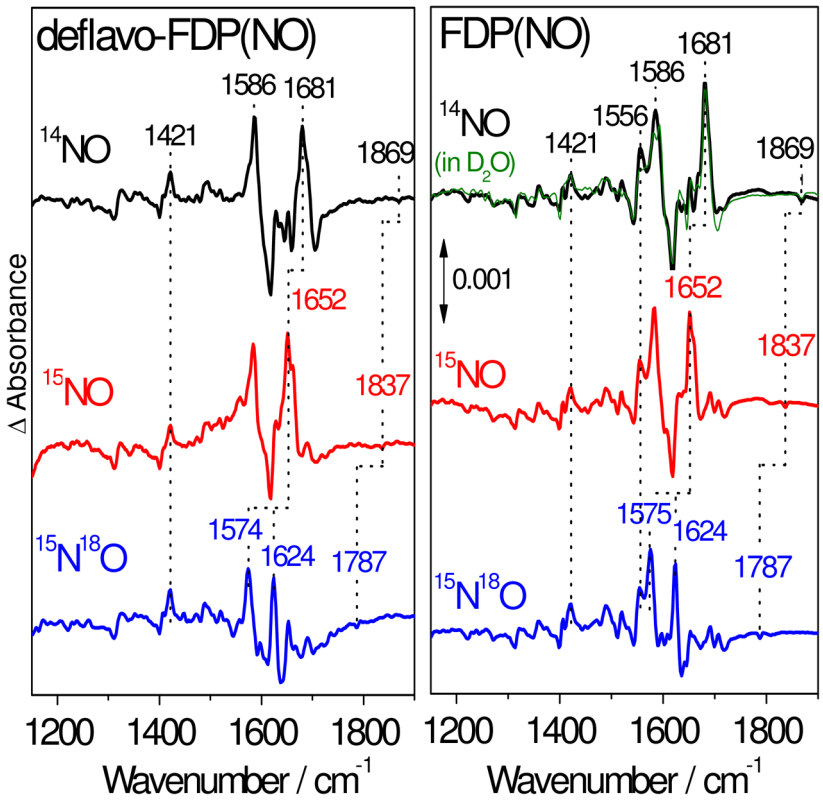

Figure 6.
FTIR dark minus illuminated difference spectra of deflavo-FDP(NO) and FDP(NO) with ^{14}NO (black), ^{15}NO (red), and $^{15}N^{18}O$ (blue) at 10 K.

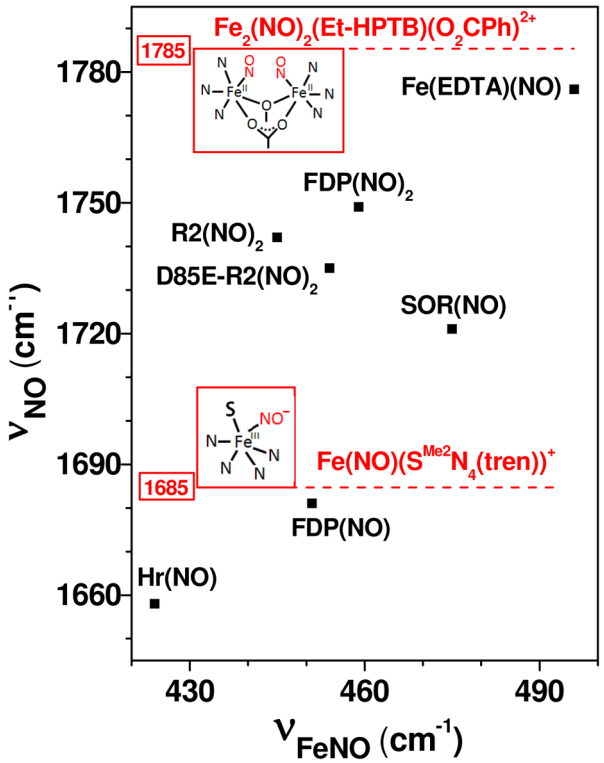

Figure 7.

ν(FeNO) vs ν(NO) plot of $S = 3/2$ nonheme $\{FeNO\}^7$ complexes and proteins (see Table 1 for frequencies and references).

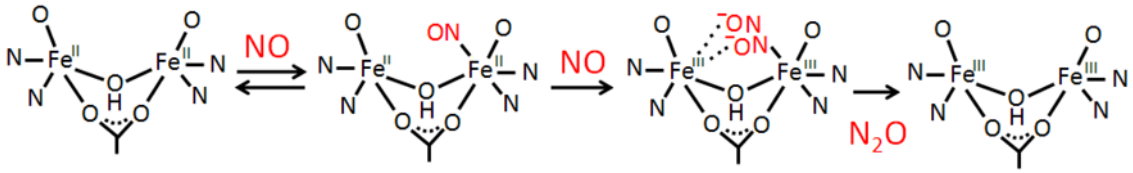

Scheme 1.
Proposed mechanism of NO reduction in FDP.

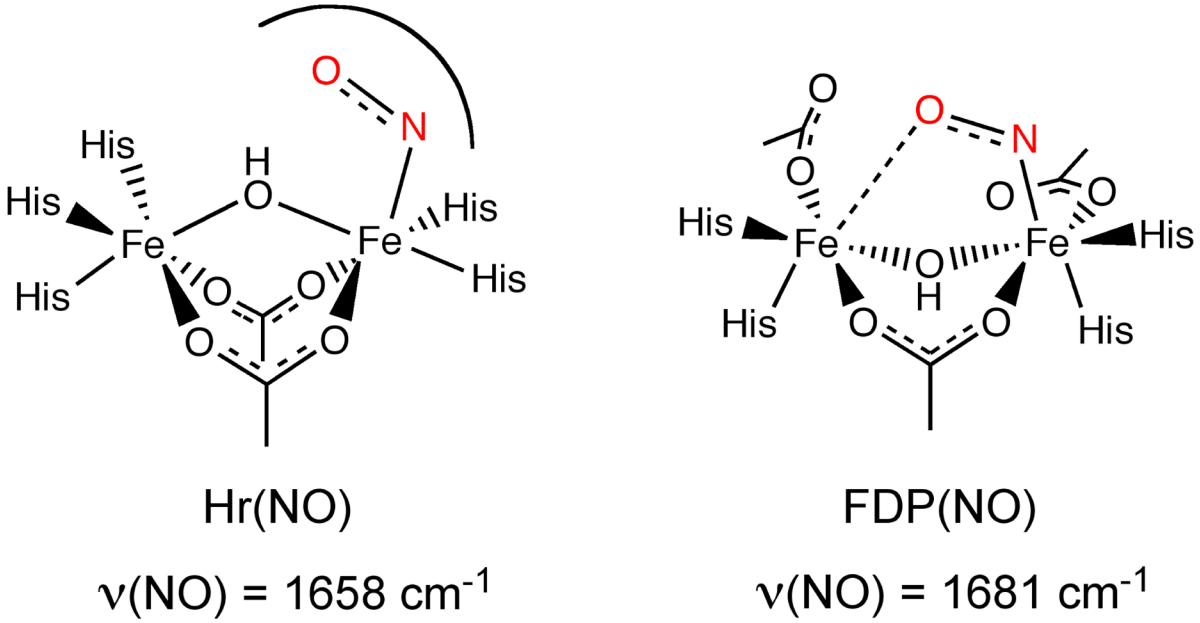

Scheme 2.
Proposed structures of the diiron mononitrosyl clusters in Hr(NO) and FDP(NO).

Table 1

Vibrational frequencies of $S = 3/2$ nonheme $\{FeNO\}^7$ species in mono- and dinuclear complexes.[a]

$\{FeNO\}^7$ species	ν(Fe-NO) ($\Delta^{15}N$) (cm^{-1})	ν(NO)	ν_s(COO-) ($\Delta^{13}C$) (cm^{-1})	ν_{as}(COO-)	$\Delta\nu_{as-s}$ (cm^{-1})	Ref.
Hr(NO)	424 (−6)	1658 (−27)[b]	1398 (−31)	1608 (−38 [b])	203[b]	This work
deflavo-FDP(NO) & FDP(NO)	451 (−9)	1681 (−29)	1421	1586	165	This work
deflavo-FDP$(NO)_2$	459 (−7)	1749 (−30)	-		-	9
R2$(NO)_2$	445 (−7)	1742 (−29)	-		-	13
SOR(NO)	475 (−7)	1721 (−31)	-		-	26
Fe(EDTA)(NO)	496 (−4)	1776 (−37)	-		-	9,10
$Fe_2(NO)_2$(Et-HPTB)$(O_2CPh)^{2+}$		1785 (−34)				24
Fe(NO)$(S^{Me2}N_4(tren))^+$		1685 (−45)				25

[a] R2 = ribonucleotide reductase R2 protein, SOR = superoxide reductase, EDTA = ethylenediamine tetra-acetate, Et-HPTB = *N,N,N′,N′*-tetrakis(*N*-ethyl-2-benzimidazolyl-methyl)-1,3-diaminopropane, O_2CPh = benzoate, $S^{Me2}N_4$(tren) = 3-mercapto-3-methyl-2-butanone, tris(2-aminoethyl)amine

[b] Based on frequencies obtained with ^{13}C-Hr(NO)

J Am Chem Soc. Author manuscript; available in PMC 2013 April 18.